Ecological Monographs, 72(2), 2002, pp. 185–202

DYNAMICS OF MEASLES EPIDEMICS: SCALING NOISE, DETERMINISM, AND PREDICTABILITY WITH THE TSIR MODEL

BRYAN T. GRENFELL,[1,4] OTTAR N. BJØRNSTAD,[2] AND BÄRBEL F. FINKENSTÄDT[1,3]

[1]*Department of Zoology, University of Cambridge, Cambridge CB2 3EJ UK*
[2]*Departments of Entomology and Biology, 501 ASI Bldg., Pennsylvania State University, University Park, Pennsylvania 16802 USA*
[3]*Department of Statistics, University of Warwick, Coventry CV4 7AL UK*

Abstract. Two key linked questions in population dynamics are the relative importance of noise vs. density-dependent nonlinearities and the limits on temporal predictability of population abundance. We propose that childhood microparasitic infections, notably measles, provide an unusually suitable empirical and theoretical test bed for addressing these issues. We base our analysis on a new mechanistic time series model for measles, the TSIR model, which captures the mechanistic essence of epidemic dynamics. The model, and parameter estimates based on short-term fits to prevaccination measles time series for 60 towns and cities in England and Wales, is introduced in a companion paper. Here, we explore how well the model predicts the long-term dynamics of measles and the balance between noise and determinism, as a function of population size. The TSIR model captures the basic dynamical features of the long-term pattern of measles epidemics in large cities remarkably well (based on time and frequency domain analyses). In particular, the model illustrates the impact of secular increases in birth rates, which cause a transition from biennial to annual dynamics. The model also captures the observed increase in epidemic irregularity with decreasing population size and the onset of local extinction below a critical community size. Decreased host population size is shown to be associated with an increased impact of demographic stochasticity. The interaction between nonlinearity and noise is explored using local Lyapunov exponents (LLE). These testify to the high level of stability of the biennial attractor in large cities. Irregularities are due to the limit cycle evolving with changing human birth rates and not due to complex dynamics. The geometry of the dynamics (sign and magnitude of the LLEs across phase space) is similar in the cities and the smaller urban areas. The qualitative difference in dynamics between small and large host communities is that demographic and extinction–recolonization stochasticities are much more influential in the former. The regional dynamics can therefore only be understood in terms of a core–satellite metapopulation structure for this host–enemy system. We also make a preliminary exploration of the model's ability to predict the dynamic consequences of measles vaccination.

Key words: attractor evolution; core–satellite metapopulation; epidemic birth–death process; extinction–recolonization; nonlinear stochastic dynamics; persistence thresholds; population cycles; time series analysis; transience; TSIR model; vaccination.

INTRODUCTION

A key issue in population dynamics is the relative importance of low-dimensional nonlinear deterministic forces and the, often high-dimensional, irregularities which we label as stochasticity (May 1973, Royama 1992, Ellner and Turchin 1995, Sugihara 1995, Stenseth et al. 1996, Leirs et al. 1997). To tease out the relative impact of these effects, we ideally need systems in which the impact of the low-dimensional forces are well understood, and where the components of the process noise, demographic stochasticity and low- or high-frequency environmental forcing, can be separated. Demographic noise is the child of discreteness and therefore scales with population size, so that an ideal system would allow us to titrate the effects of demographic uncertainty at a range of population sizes subject to the same dynamical forces. Finally, we need both rich data sets and relatively straightforward dynamical descriptions of them in order to integrate observations and models properly. Here we build on the model and parameter estimates of our previous paper (Bjørnstad et al. 2002) to propose that the dynamics of childhood infections, notably measles, in developed countries provide one of the best available test beds for exploring these issues. Specifically, we explore how the long-term dynamics of measles epidemics depends on the balance between nonlinear epidemic forces, demographic noise, and environmental forcing, and how these dependencies scale with host population size.

The balance between noise and determinism is intimately linked to another key issue: the level of predictability of ecological systems. Establishing the lim-

Manuscript received 5 July 2000; revised 13 April 2001; accepted 30 April 2001.
[4] E-mail: b.t.grenfell@zoo.cam.ac.uk

its to quantitative dynamical prediction, set by stochastic uncertainties or deterministically chaotic forces, can teach us about a system's dynamics, and reveal the temporal scale at which forecasting is reliable (Sugihara et al. 1990, Sugihara and May 1990, Tong 1990, Ellner and Turchin 1995). Qualitative predictive ability, the presence or absence of oscillations, for example, is also an important test of models; especially when this refines our understanding of underlying biological mechanisms. A particularly hard test of models is provided by a characteristic feature of many ecological time series: transitions between different dynamical behaviors through time or space (e.g., Murdoch and McCauley 1985, Stokes et al. 1988, Stenseth et al. 1996, Bjørnstad et al. 1998, Finkenstädt and Grenfell 1998). Teasing out whether these changes arise from internal dynamics (such as intermittent periodicity associated with chaos; Kendall et al. 1993, Schaffer et al. 1993), or secular changes in important parameters (such as transitions in vital rates; Stokes et al. 1988, Finkenstädt and Grenfell 1998) is a key task for population dynamics (Sugihara 1995). Mechanistic and semimechanistic models (Ellner et al. 1998) are particularly powerful here, if they can allow for the consequences of known changes in the system's parameters (Finkenstädt and Grenfell 2000). This form of prediction can have an important applied dimension since such shifts are often directly or indirectly anthropogenic in origin; relating, for example, to the effects of global warming (Fan et al. 1998) or vaccination (Anderson and May 1991).

Validation of predictive models requires data against which to test assumptions and predictions. Since the results of large-scale experimental manipulations at the population level are generally not available to ecologists, a common strategy is to fall back on ''postdiction'' of historical time series. Childhood infections, notably measles, provide a paradigm for this form of prediction (Sugihara et al. 1990, Tidd et al. 1993, Grenfell et al. 1994, 1995, Ellner 2000, Finkenstädt and Grenfell 2000, Grenfell 2000; Finkenstädt et al. 2002). Pre- and postvaccination measles notification data sets are extensive (Grenfell and Harwood 1997) and there is a firm theoretical understanding of both the deterministic (Anderson and May 1991) and stochastic (Bartlett 1956) underpinnings of measles epidemics.

We use the time series SIR (TSIR; Time series Susceptible–Infected–Recovered) models to bridge the gap between epidemiological data and models. In the companion paper (Bjørnstad et al. 2002), we develop the model, estimate its parameters, and study how the parameter estimates scale with host population size. In this paper, we focus mainly on the long-term dynamics of measles. We first show how the TSIR model successfully represents the typically observed biennial predator–prey like alternation of infected and susceptible individuals; the cycle is maintained by a seasonally varying infection rate (Schenzle 1984). We subsequently use the model to understand how stochasticity, virus transmission, and secular changes in birth rates interact to modulate the epidemic dynamics. The model captures the essential features of comparative long-term prevaccination dynamics of measles, across a range of cities in England and Wales, spanning three orders of magnitude in size. For large cities, where measles is endemic, seasonal variations in contact rate and longer-term variations in birth rate are sufficient to describe these dynamics. In smaller centers, below a critical community size (CCS) of ~300 000–500 000 (Bartlett 1960), demographic stochasticity and extinction/recolonization become increasingly important. Decreasing host population size thus induces two critical transitions: (1) local dynamics changes from regular and predictable cycles to more stochastic outbreaks and (2) persistence changes from a local level to the metapopulation level. We reach these broad conclusions by addressing the following more specific issues:

1) How predictable is the, generally biennial, alternation of major and minor epidemics in large cities in the prevaccine era, and what is the impact of long-term trends in birth rate on these patterns?

2) How does predictability change with the progression from regular endemic disease oscillations in large cities above the CCS (Bartlett's [1960] type I dynamics), through regular epidemics with intervening fadeouts in smaller urban centers (type II dynamics), to more irregular (type III) dynamics in still smaller centers?

3) How does the importance of stochasticity scale with population size? And, how does the interaction between ''noise'' and nonlinear regulation determine the transition from regular endemic cycles in large cities, to episodic epidemics in small towns? We approach this through a combined discussion of local Lyapunov exponents (LLE; Bailey et al. 1997) and stochastic forcing.

In the *Results* section, we focus mainly on using the TSIR model to titrate the relative impact on measles dynamics of stochastic and deterministic forces and the resulting implications for qualitative and quantitative dynamic predictability. In the *Discussion,* we explore the wider ecological implications of this methodology and its application.

Materials and Methods

The data

We use official weekly notification data for measles, and associated demographic data, for 60 towns and cities in England and Wales between 1944 and 1994; a full description of the structure and limitations of the data set is given by Bjørnstad et al. (2002). We focus mainly on the prevaccination era (1944–1966). The raw data for the 60 cities—the biweekly incidences of measles and the annual data on human birth rates—are available online from the Department of Zoology at

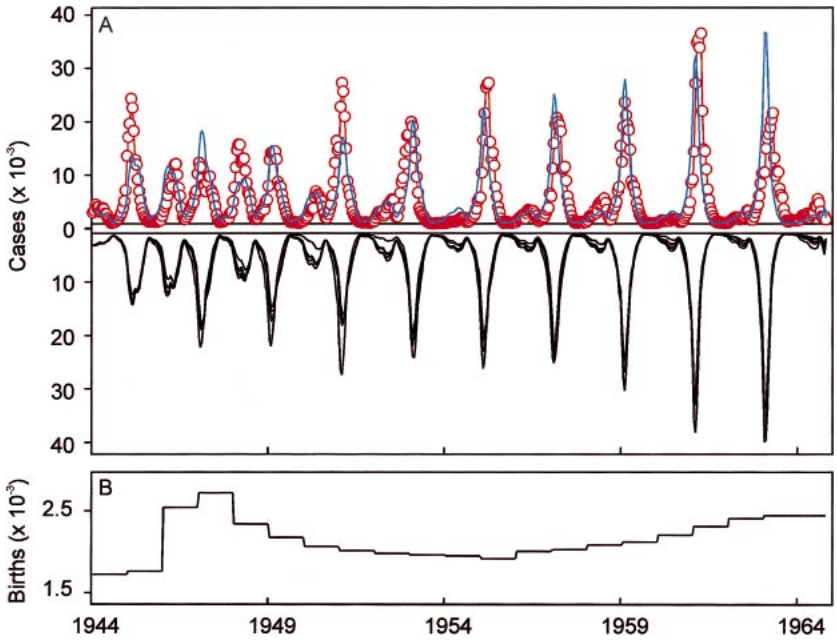

FIG. 1. (A) Measles incidence in 2-wk periods (in hundreds) in London from 1944 to 1965. The circles and the red line represent observed incidence (corrected for underreporting). The blue line represents the deterministic prediction from the TSIR model (using the susceptible and infected density in the first 2-wk period of 1944 as initial conditions). The black lines (and inverted scale) represent five stochastic realizations of the TSIR model. (B) The biweekly number of births (in hundreds) in London. The numbers are averaged within each year. The post-World War II baby boom in the late 1940s is associated with a period of annual cycles in measles incidence.

Cambridge University.[5] Figs. 1 and 2 show epidemic trajectories for 12 representative cities spanning the range from the largest (London, 3.3×10^6 people) to the smallest (Teignmouth, 10 500 people) host communities. Bartlett (1960) classified the fluctuations in measles incidence as type I dynamics (regular endemic oscillations in large cities, above ~250 000 inhabitants), type II dynamics (regular epidemics with intervening fadeouts in smaller urban centers), and type III dynamics (irregular outbreaks with long fadeout periods in small towns and villages). Fig. 2 is arranged such that rows one through three represent type I through III dynamics, respectively. Bjørnstad et al. (2002: Fig. 2) illustrate how the transition in type of dynamics is associated with increasing frequency of local extinction: type I cities never (or only extremely rarely) exhibit local extinctions while type III cities may exhibit measles extinction a third of the time (or more). A preliminary analysis of the pattern of local extinctions in the full England and Wales measles database (1400 locations) indicates a smooth transition from type II to type III in the length and frequency of local extinctions (Grenfell and Bolker 1998). Note therefore that the above choice of type II and III cities is relatively subjective, however it does illustrate the observed change in dynamics with population size, for comparison with the model.

[5] URL: ⟨http://www.zoo.cam.ac.uk/zoostaff/grenfell/measles.htm⟩

The TSIR model

This is a discrete-time nonlinear stochastic analogue of the well-known SIR (Susceptible–Infected–Recovered) model (Dietz and Schenzle 1985, Anderson and May 1991, Finkenstädt and Grenfell 2000, Bjørnstad et al. 2002). It is also closely related to the chain binomial model (e.g., Bailey 1957; see *Discussion* in Bjørnstad et al. 2002). The model thus builds on both the distinguished literatures of theoretical and statistical epidemiology. The characteristic time scale of the chain is 2 wk (corresponding roughly to the sum of incubation and infectious periods for the infection; Anderson and May 1991). We denote the number of resident infectious host at time t ($t = 1, \ldots, T$) by I_t, and the number of epidemic imports (immigrant infections) by θ_t. The force of infection, the infection pressure experienced by one susceptible individual, can then be expressed as $\beta_s(I_t + \theta_t)^\alpha$, where β_s is the per capita transmission rate; α allows for nonlinearities in contact rates (Liu et al. 1987; see also *Discussion*). The expected number of cases in the next time step (the epidemic intensity) is then assumed to be

$$\lambda_{t+1} = \beta_s(I_t + \theta_t)^\alpha S_t \qquad (1)$$

where S_t is the number of susceptible hosts. In the companion paper (Bjørnstad et al. 2002), we discuss all the estimated parameters, and their associated uncertainty, in detail. A crude summary of the results are as follows: the per capita transmission rate varies sea-

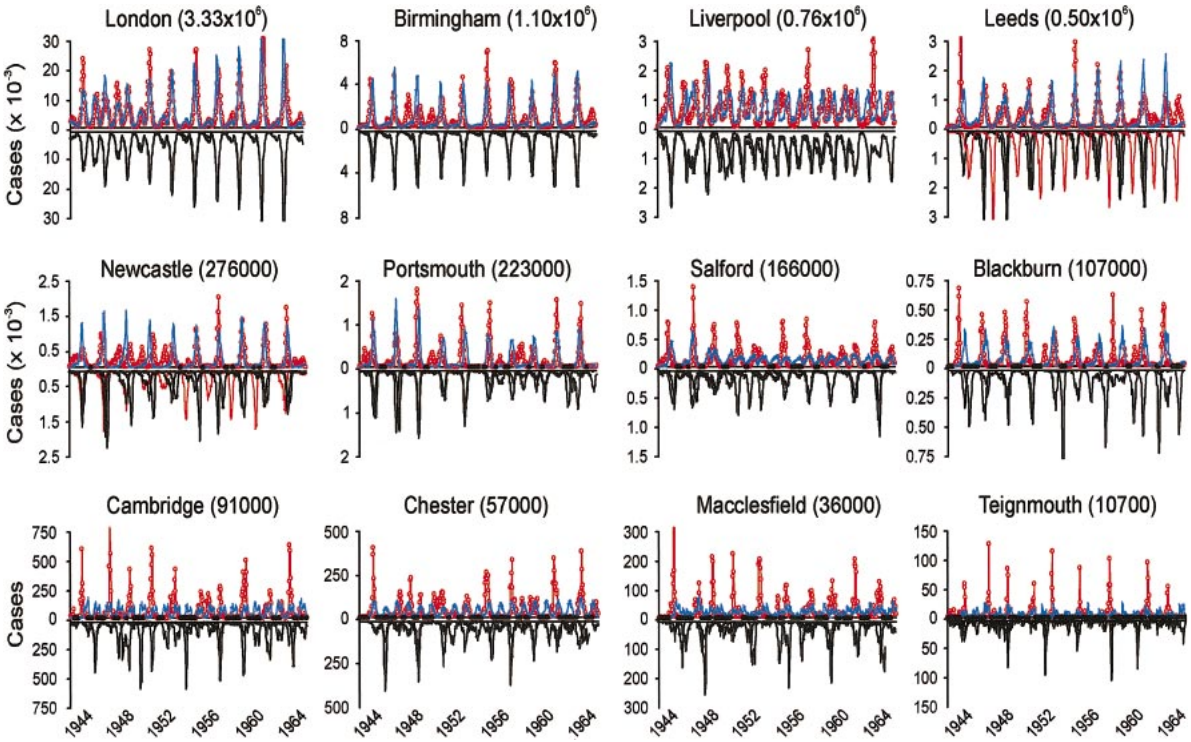

FIG. 2. Measles incidence (in hundreds) in 12 representative cities/towns spanning the population range from large cities (London, 3.3×10^6) to small urban areas (Teignmouth, 10 500 inhabitants) in the United Kingdom from 1944 to 1965. Circles and red line represents observed incidence (corrected for underreporting). The black dots along the abscissa represent 2-wk periods of local extinction. The blue line represents the deterministic prediction from the TSIR model. The black lines (and inverted scale) represent five stochastic realizations of the TSIR model (cf. Fig. 1 legend). For two of the cities (Leeds and Newcastle) we have highlighted (in red) stochastic trajectories that have jumped onto the even-year attractor. The top row comprises four large cities that represent type I cities (sensu Bartlett 1960) with endemic cycles. The second row represents four type II cities that exhibit regular epidemics interspersed by short fadeout periods. The bottom row depicts the irregular epidemics of four different type III cities.

sonally because of school-term forcing (the realized per capita transmission rate is higher during school term than during school holidays). Fig. 3a depicts the seasonal transmission rate, as estimated on the basis of the measles data for London (see Fig. 1). Over and above the seasonal variation, however, the mean per capita transmission rate is inversely proportional to host community size (see Bjørnstad et al. 2002: Fig. 7a and Eq. 6). This essentially corresponds to frequency-dependent transmission (or ''true mass action'' sensu de Jong et al. 1995, McCallum et al. 2001). The mixing coefficient, α, is shown to vary somewhat, but it is nearly independent of host community size and very close to unity (Bjørnstad et al. 2002: Fig. 6); indicating approximate homogenous mixing. Note, though, that analyses presented by Finkenstädt and Grenfell (2000) suggest that α is typically slightly lower than unity (see also Finkenstädt et al. 2002).

Another key stochastic process is the transfer of infection between towns. The TSIR model uses, as a first approximation, the assumption that the influx rate of infection, θ_t, follows a Poisson process with time-invariant mean m:

$$\theta_t \sim \text{Poisson}(m) \tag{2}$$

where ''$\sim$'' is shorthand for ''is distributed as.'' Following detailed analysis under the assumption of timeinvariance, uncertainty in the estimation of θ still prevails. We will, nevertheless, (but tentatively) use the estimates presented in the companion paper (Bjørnstad et al. 2002) for further analysis. This analysis indicates that m increases with city size, but slower than linearly (as conjectured by Bartlett 1966).

Eq. 1 follows directly from the extensive theoretical literature on childhood-disease dynamic modeling (see reviews in Anderson and May 1991, Grenfell and Dobson 1995, Mollison 1995). In order to make a comprehensive model for measles dynamics, we also need to consider the demographic stochasticity inherent from births and deaths in any ecological system (Kendall 1949, Bartlett 1956, see also Renshaw 1991). In the absence of such variation, the number of new cases, I, would be identical to the epidemic intensity, λ, according to

$$I_{t+1} = \lambda_{t+1}. \tag{3a}$$

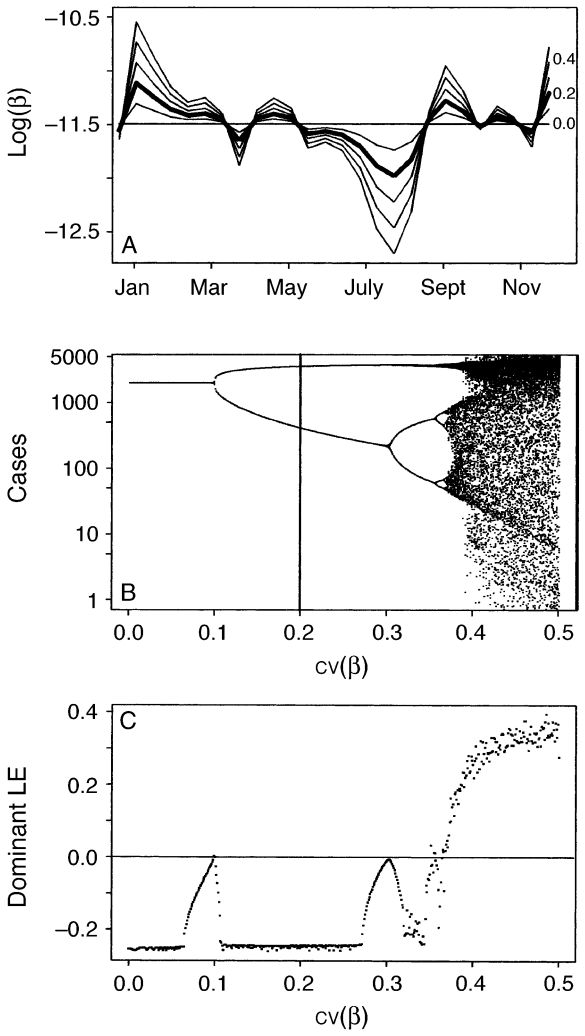

FIG. 3. The effect of seasonal variation on measles dynamics. (A) The bold line signifies the seasonal cycle in log-transmission rate, Log(β), in London (see Bjørnstad et al. 2002: Fig. 7). The estimated coefficient of variation (CV) in β is 0.20. The variation is caused by term-time aggregation of school children and age-structured heterogeneities (see also Earn et al. 2000). The superimposed lines represent analogous seasonal cycles corresponding to a seasonal CV of 0 (i.e., no seasonal forcing), 0.1, 0.3, 0.4, and 0.5. (B) The bifurcation diagram of measles incidence against CV(β). In order to highlight multiannual fluctuations, incidences are summed across individual years; single lines, thus, represent an annual cycle, the two branches represent the biennial cycle, etc. The bifurcation plot spans 200 yr (= 5200 generations) after a transient period of 10 yr. The annual cycle bifurcates into a biennial cycle at CV(β) = 0.1, which further bifurcates at CV(β) = 0.3. The vertical line represents the seasonal CV observed in London. (C) The Lyapunov exponent of the skeleton TSIR model against annual CV(β) as estimated from the time series in (B). Measles dynamics are predicted to go chaotic as the CV exceeds 35%.

We will refer to Eq. 1 and Eq. 3a as the deterministic skeleton formulation.

In the presence of demographic stochasticity, however, the dynamics will not be realized according to the deterministic skeleton. Using the locally constant approximation to the nonlinear birth–death process (Bjørnstad et al. 2002), the number of infected individuals after one characteristic time unit (~2 wk for measles) will be realized according to

$$I_{t+1} \sim \text{NB}(\lambda_{t+1}, I_t) \tag{3b}$$

where NB(a, b) signifies a negative binomial distribution, with expectation a and clumping parameter b. We will refer to Eqs. 1, 2, and 3b as the (doubly) stochastic formulation. Note that $\{I_t\}$ is now a sequence of discrete integer variables, in contrast to the continuous epidemic intensity of the deterministic formulation.

There are two additional issues we need to address: susceptible replenishment and environmental forcing on the susceptible dynamics due to secular changes in the vital rates of the human host (Finkenstädt and Grenfell 1998, 2000, Finkenstädt et al. 1998, 2002). Both of these can be incorporated in a simple balance equation for the susceptibles:

$$S_{t+1} = S_t + B_t - I_{t+1} \tag{4}$$

where B_t represents the number of births. The annual per capita birth rates of humans ranges from ~0.01 to 0.02 in Britain in the decades following World War II (Office of Population Censuses and Surveys; OPCS). The birth rates, however, vary geographically (Liverpool, for instance, has relatively high rates) and temporally (the post-World War II baby boom resulted from a 30% increase in birth rates as compared to prior and posterior periods; Finkenstädt and Grenfell 1998). We will refer to Eqs. 1–4 as the TSIR model. Full details on the parameter estimation are given in Bjørnstad et al. (2001).

In summary, we note that Eqs. 1–3 predict the mean infection intensity for the next time step (λ_{t+1}) as a function of (1) the numbers of current infective and susceptible individuals (I_t and S_t, respectively), modified by the "mixing exponent" (α) which allows for nonlinearities in transmission; (2) seasonal variations in transmission, β_s (Fig. 3a); (3) a Poisson-distributed influx of infection from other places, θ_t; and (4) the susceptible balance equation, wherein the number of host births may vary through time.

Dynamics

In order to understand the dynamics of measles across the range of host community sizes, we analyze both the deterministic skeleton of the TSIR model and the full stochastic dynamics. The former situation is given by Eqs. 1, 2, 3a, and 4; in this case we either (for cities above CCS) assume the stochastic influx, θ_t, to be negligible (i.e., $\theta_t = 0$ for all t) or take the influx

to be a time-invariant constant ($\theta_t = m > 0$ for all t). The latter stochastic dynamics are defined by the doubly stochastic model given by Eqs. 1, 2, 3b, and 4.

We can use the estimates of the susceptible and infected density in the first 2-wk period of 1944 (S_0, I_0) as initial conditions for simulations. The latter is directly reported but has to be calibrated for underreporting (Finkenstädt and Grenfell 2000). The former is estimated from susceptible reconstruction (Finkenstädt and Grenfell 2000, Bjørnstad et al. 2002). Given the city-specific epidemiological parameters (Bjørnstad et al. 2002), we then study the sequence of subsequent measles epidemics, either deterministically or stochastically. Unless otherwise stated, all simulations use the city- and time-specific birth rates. We use repeated Monte Carlo simulations of the model and compare the results with the data. Unless otherwise stated, the stochastic behavior is a summary across 10 000 realizations of each model (all starting from the observed initial conditions). In particular, we focus on how well the (1) simulated trajectories, (2) spectral densities, and (3) critical community size and fadeout lengths match the observations. We further analyze how community size affects the rate of stochastic divergence in epidemic trajectories. We use the periodogram on square-root transformed case counts to estimate the spectral densities (Priestley 1982).

Lyapunov exponent, control parameters, and bifurcation

In order to explore the short-term predictability of measles, and the interaction between stochastic and regulatory forces on measles dynamics, it will be useful to consider the sensitivity of the dynamics to small differences in initial conditions (such as those that may arise from demographic stochasticity). This sensitivity is commonly quantified by the dominant Lyapunov exponent. There are a number of important conceptual and methodological issues pertaining to this measure as applied to stochastic systems (Bailey et al. 1997, Tong 1997). We measure the dominant Lyapunov exponent (LE) of the deterministic skeletons by using the Jacobian method as developed by Bailey et al. (1997; see also Eckmann et al. 1986). That is, we define the finite time LE as follows:

$$\mathrm{LE} = \frac{1}{T}\log\left\|\left(\prod_{t=1}^{T}\mathbf{J}_t\right)\mathbf{U}_0\right\| \qquad (5)$$

where Π represents matrix premultiplication, $\|\cdot\|$ represents the vector norm, and $\mathbf{U}_0$ is a unit length vector. We use $\mathbf{U}_0 = \binom{1}{0}$ (see Bailey et al. 1997). The matrix $\mathbf{J}_t$ is the Jacobian of the deterministic skeleton of the epidemic model

$$\mathbf{J}_t = \begin{pmatrix} \alpha\beta_s S_t(I_t + \theta_t)^{\alpha-1} & \beta_s(I_t + \theta_t)^{\alpha} \\ -\alpha\beta_s S_t(I_t + \theta_t)^{\alpha-1} & 1 - \beta_s(I_t + \theta_t)^{\alpha} \end{pmatrix}. \qquad (6)$$

As a crude measure of the dominant (global) Lyapunov exponent, we calculate LE on the basis of 100 yr (2600 iterations of the model) after discarding the first 2600 iterations. There are two control parameters that are important in our study: first, the amount of seasonality (as measured, for example, by the coefficient of variation of β across the annual cycle), and, second, the rate of susceptible replenishment (i.e., the birth rate, B). Fig. 3b and c illustrate how the seasonality in β controls the stability of the skeleton; as seasonal variation increases, the dynamics undergo a transition in dynamics from an annual cycle, through a biennial cycle to multiannual oscillations and chaos for high degrees of seasonality. The parameter estimates presented in the companion paper testify that London measles resided in the biennial part of parameter space during the prevaccination era. Finkenstädt and Grenfell (2000) and Earn et al. (2000) discuss the effect of birth rates on measles dynamics and show that increased rates result in a collapse of the biennial attractor onto an annual cycle. In contrast, decreased birth rates result in complex coexisting attractors in the seasonally forced SEIR (Susceptible–Exposed–Infectious–Recovered) model (Earn et al. 2000). This appears also to be the case for the TSIR model, albeit only for values of α close to 1 (K. Glass and B. Grenfell, *unpublished manuscript*).

In order to dissect the interaction between noise and nonlinear regulation we need to understand how the relative noise level changes during the epidemic. In the companion paper (Bjørnstad et al. 2002), we show that the birth–death process results in a coefficient of variation in the dynamics that changes through the cycle according to: $\mathrm{CV}(t) \approx \sqrt{2/I_t}$. We will use the one-step-ahead local Lyapunov exponent, LLE, to understand how this demographic stochasticity is amplified or reduced through the epidemic cycle. We follow Ellner et al. (1998) and Bailey et al. (1997), and study the one-step-ahead LLE evaluated at each point along the epidemic trajectory.

Noise-induced divergence may be particularly rapid in the presence of coexisting attractors because randomness may shift a population from one attractor onto another (e.g., Earn et al. 2000). In the face of an annual cycle, there is just a single attractor. In contrast, the biennial regime exhibits two coexisting attractors that differ only with respect to whether the major peak falls in the odd or the even year (see Henson et al. 1998 for a related discussion). In the *Discussion*, we consider the TSIR model's depiction of more complex coexisting attractor structures for measles.

Results

Measles dynamics in big cities

We begin by considering what the TSIR models tell us about the balance between noise and determinism in large centers, as epitomized by London. Fig. 1a shows observed prevaccination dynamics in London

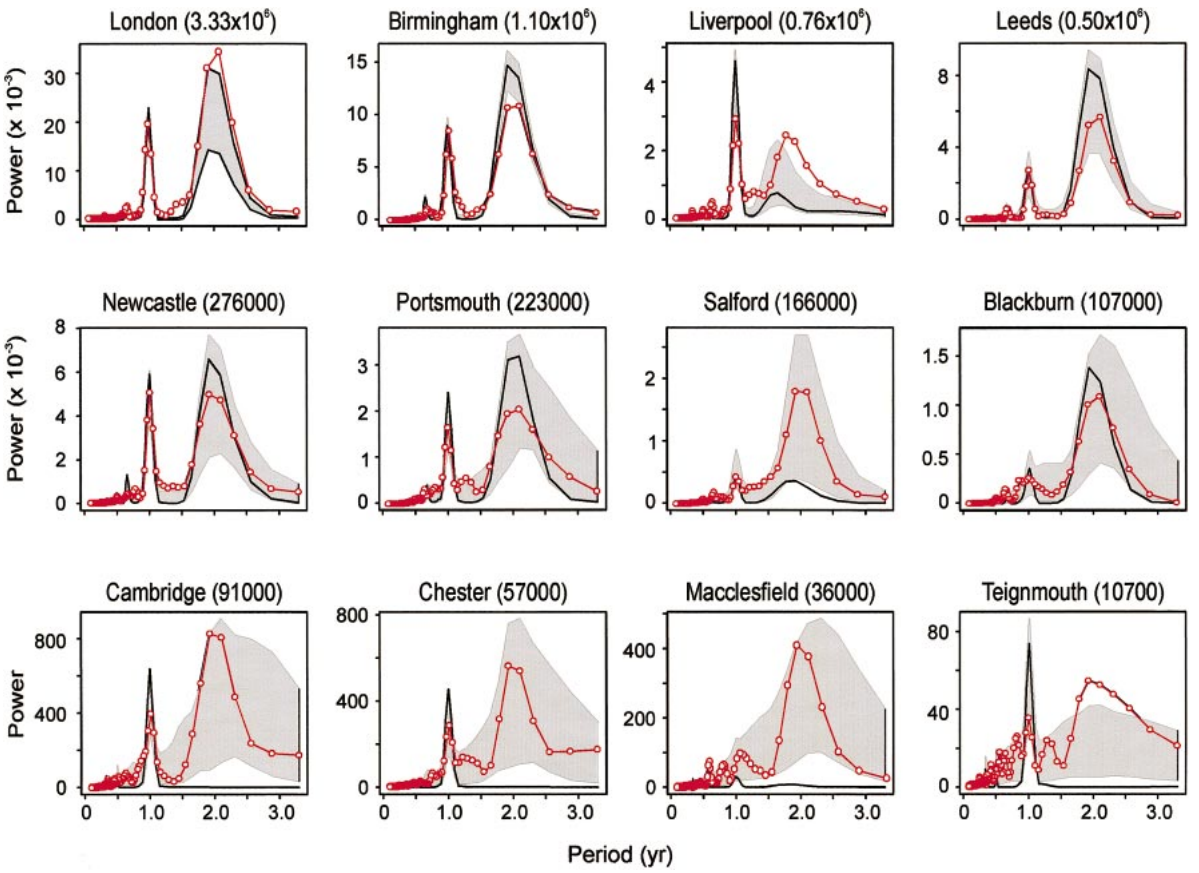

FIG. 4. Power spectra (in hundreds) of measles for the 12 representative cities/towns (cf. Fig. 2) in the United Kingdom from 1944 to 1965. The circles and the red lines represent the power spectra of the observed incidence (corrected for underreporting). The black line represents the spectrum of the deterministic prediction from the TSIR model. The gray envelopes represent 95% envelopes across 10 000 stochastic realizations of the TSIR model.

(1944–1966), corrected for underreporting (Finkenstädt and Grenfell 2000). Superimposed on the observed case counts are simulations of the deterministic skeleton (hereafter deterministic) TSIR model and five replicate simulations of the stochastic model allowing for demographic noise (for clarity, the latter are plotted on an inverted scale). A number of key results emerge from simple visual inspection of this figure.

1. *Predictable major epidemics*.—Measles incidence exhibit conspicuous fluctuations that have both an annual and a biennial component (Finkenstädt and Grenfell 2000). In London, the annual component is more dominant in the early part of the series, whereas the biennial component predominates the second half (see next paragraph). As reviewed above, these cycles arise from the interaction of time-delayed density-dependent epidemic dynamics, ''forced'' by the external seasonal driver of school terms. The figure spans 21 yr of data, which represents ~550 ''measles generations.'' The visual correspondence between the data and the model prediction is encouraging; the correlation between the data and the deterministic ''postdiction'' (on variance-stabilized, square-root-transformed data) is 0.84 over the 20 yr. (Recall also that the one-step-ahead fit of the model to the data, essentially 2-wk-ahead predictions, was 0.98; Bjørnstad et al. 2002). Note, though, that the simulation does not represent true out-of-sample prediction (we return to this in the *Discussion*).

2. *Dynamic transitions*.—In addition to capturing the overall trajectory of the epidemic, the TSIR simulations also closely match the clear transition in measles dynamics—from relatively low amplitude annual epidemics in the 1940s, to large, predominantly biennial, outbreaks from ~1950. This transition has been studied in detail (Finkenstädt and Grenfell 1998, 2000, Finkenstädt et al. 1998, Earn et al. 2000). The current understanding is that the baby boom in the second half of the 1940s increased the production of susceptibles (Fig. 1b) to the extent that the dynamics collapsed onto an annual attractor. This collapse was released as birth rates dropped in the early 1950s.

3. *Impact of demographic noise*.—The forecasting for London measles incidence is largely unaffected by including the demographic stochasticity inherent in the epidemic process (Fig. 1a). The mean correlation be-

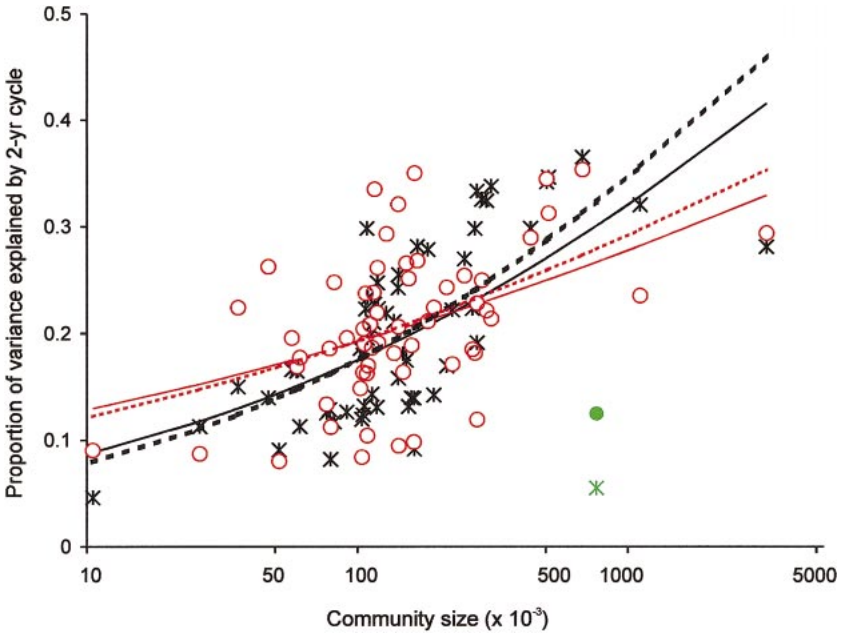

FIG. 5. The proportion of the total variation captured by the 2-yr peak of the power spectra (see Fig. 4) plotted against community size (logarithmic axis). The power of the 2-yr peak is summed across the frequencies 0.018 and 0.020 (corresponding to 2.1- and 1.9-yr periods). Red circles represent the observed proportions; black crosses represent the predicted proportions from the stochastic TSIR model (mean across 10 000 realizations). Liverpool (and its dominance of annual fluctuations) is highlighted in green. The full red line is the logistic regression of observed proportions against log community size ($F_{1,58} = 13.7$, $P < 0.01$). The full black line is the corresponding logistic regression for predicted proportions ($F_{1,58} = 37.1$, $P < 0.01$). Dotted lines are logistic regressions after omitting Liverpool.

tween the data and the stochastic ''postdiction'' (using variance stabilized, square-root-transformed data) is 0.83, while that between the deterministic and the stochastic trajectories is 0.98. The absence of stochastic divergence is further testified to by the close correspondence between the different stochastic trajectories (the mean correlation between them is 0.97). Note, however, that the simulations in Fig. 1a are not identical—there is variation, especially at major and minor epidemic peaks.

One reason for the absence of stochastic divergence is the scaling of demographic noise with host community size (one disease-generation ahead CV $\approx \sqrt{2/I_t}$). For London, the largest city in the the United Kingdom, this scaling results in a mean CV of 3.9%. The CV is largest in the troughs, where it rises as high as 14.4% (the incidence rarely drops below 100 individuals in the prevaccination era). However, across most of the cycle the demographic noise is negligible (CV $>$ 10% for a mere 4.3% of the time). The short-term (2-wk period to 2-wk period) effect of demographic stochasticity is therefore relatively weak. However, as we shall discuss in more detail later, this scaling of demographic noise is not the full story. In a linear stochastic system, even weak noise would be compounded through time to cause complete stochastic divergence, since such dynamics are ''phase-forgetting'' (sensu Nisbet and Gurney 1982). In order to understand the predictability of the current system, we also need to study the nonlinear (density-dependent) amplification/reduction of noise through the epidemic cycle.

Overall, however, the TSIR model ''postdicts'' the London data remarkably well for an ecological model of a microparasite ''in the wild.'' We now turn to how this fit between theory and data scales with host abundance (i.e., human community size).

Measles dynamics and population size: historical trajectories

In Fig. 2 we extend the London analysis (Fig. 1) to 12 representative urban areas. The top row comprises four of the largest cities in the England and Wales (again including London). These are all type I cities (sensu Bartlett 1960) that exhibit endemic cycles. The second row represents a selection of type II cities that exhibit regular epidemics interspersed by short fadeout periods. The last row depict the irregular epidemics of type III cities. The simulated series capture qualitatively the major epidemic dynamics across time over the range of population sizes. A visual inspection, however, reveals a number of interesting features about the dynamics (most of which we will return to in the paragraphs following this initial inspection) of the three types of cities:

1) Type I cities (Fig. 2, top row) exhibit dynamics that are quantitatively well predicted by both deterministic and stochastic simulations; measles is predicted to be endemic, and both the biennial dynamics

of Birmingham and Leeds and the annual fluctuations in Liverpool are captured by the model. Note, however, how one of the stochastic realizations for Leeds is locking onto the even-year attractor and thus drifting perfectly out of synchrony with the other (odd-year) trajectories.

2) Type II cities (Fig. 2, row 2) are predicted to exhibit fairly regular epidemic cycles, interspersed by short fadeout periods. The four cities depicted are observed (compared to corresponding stochastic prediction ± 1 SD) to have measles extinction 2.3% (3.1% ± 0.5%), 6.7% (5.5% ± 2.3%), 6.2% (2.3% ± 1.5%), and 13.1% (15.5% ± 5.3%) of the time, respectively. We will return to the pattern of extinction below. Furthermore, they exhibit intermediate scale predictability, in that the first 10 yr (i.e., 250 generations) are well predicted, but stochastic divergence is apparent thereafter. The deterministic models generally exhibit dynamics qualitatively similar to the observed dynamics and to those of the stochastic realizations.

3) Type III cities (Fig. 2, row 3) are predicted by the stochastic model to exhibit erratic epidemic outbreaks, interspersed by long periods of extinction. The four cities are observed (stochastic prediction ± 1 SD) to have measles extinction 18.6% (13.3% ± 4.8%), 29.3% (19.3% ± 6.2%), 33.7% (30.1% ± 6.5%), and 60.9% (39.4% ± 3.3%) of the time. Stochastic divergence is predicted to be fast. Overall, the amplitude and frequency of outbreaks appear to be reflected in the stochastic realizations. In contrast to the larger cities, the deterministic models fails qualitatively to predict the dynamics; deterministic models all predict measles in type III cities to have low incidence of measles with erratic annual variation. Note that the failure to capture the dynamics is despite the fact that the R^2 of the model of the short-term dynamics (measured as 1 − [residual deviance/null deviance]) are >73% in all models (Bjørnstad et al. 2002). Thus, short-term (biweekly) prediction works relatively well for small towns, whereas longer-term prediction is compromised by instability arising from stochasticity. This instability arises from a combination of demographic uncertainty (which permits local extinction of infection) and the stochastic nature of immigration (which generates variation in the waiting time before reintroduction of infection).

Measles dynamics and population size: power spectra

We can make quantitative comparisons of observed and simulated dynamics by spectral analysis. Fig. 4 shows the power spectra of observed incidence for the 12 sample cities of Fig. 2. The power spectra were calculated using the periodogram (smoothed by a Daniel window of width 3; Priestley 1982). Superimposed on the power spectra are the deterministic and stochastic spectra that are predicted by the TSIR model. As evident also from the time trajectories (Fig. 2), most of the observed spectra (black) show strong variation at annual and biennial periods, with a dominant biennial peak in power. There are two exceptions. First, Liverpool shows much stronger annual variation. Second, the smallest town, Teignmouth, shows a much wider spread of power around the 2-yr peak.

The spectra of the deterministic TSIR model are in very good agreement with the real data for large (Type I, Fig. 4, top row) and intermediate-size (Type II, Fig. 4, middle row) host communities. Note, for example, how the predominantly annual dynamics of Liverpool are predicted. Intriguingly, the deterministic modeling fails miserably for small (Type III, Fig. 4, bottom row) cities for which demographic stochasticity and extinction/recolonization dynamics are important.

The stochastic simulations highlight further important features of both the model and the dynamics (Fig. 4). First, the simulations broadly capture the observed balance between annual and biennial cycles, including the conspicuous behavior of Liverpool and Teignmouth. Second, as population size declines, the envelopes widen considerably. London (and other large cities) tends to show very similar replicate stochastic simulations (Fig. 2). The cyclic behavior become steadily more variable, both within and between simulations as population declines, as reflected in the widening frequency envelopes. Third, the fully stochastic model can capture the periodic component of the dynamics well, even in the smallest cities. Hence, the temporal patterns of fluctuations can be predicted even in small host communities where both birth–death and extinction–recolonization stochasticities are dominant. It is the exact timing and size of outbreaks that are nonpredictable.

Predictability: periodicity and city size

Measles dynamics show predominantly biennial cycles in most cities (except Liverpool). However, the dominance of this clockwork appears to depend on host community size. To summarize this across the full 60-city data set, we calculate the proportion of the variance that is accounted for by the 2-yr peak of the spectrum (Fig. 5). The proportion is found to increase significantly with community size, from ~10% for the smallest cities to ~40% for the biggest (logistic regression of proportion against log[size]: $F_{1,58} = 13.7$, $P < 0.01$). The proportion predicted by stochastic simulations is found to vary in a similar fashion (Fig. 5; logistic regression of proportion against log[size]: $F_{1,58} = 37.1$, $P < 0.01$). There is a fair amount of variation between predicted and observed proportions ($R = 0.50$, $P > 0.01$). Despite this, their relationships to community size are very similar (Fig. 5). Further analyses, based on the more regularly biennial series post-1952 (not shown), reveal a similar, but stronger, relationship between bienniality and community size.

The deterministic predictions of biennial power-ratio work well (and match the stochastic results) for the

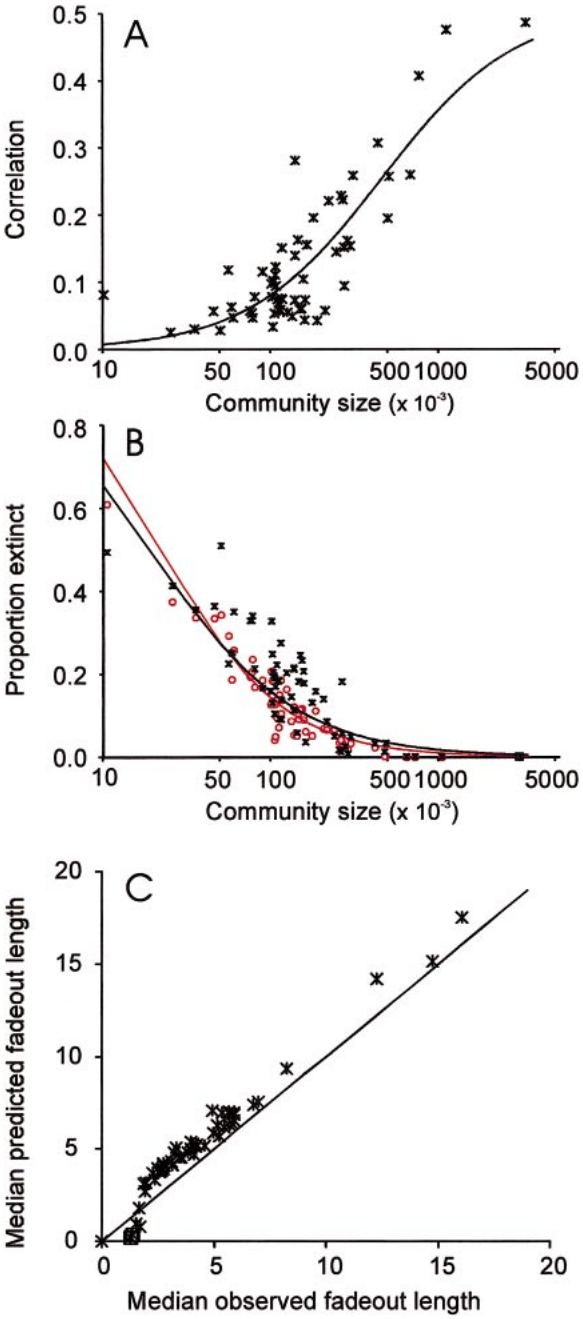

FIG. 6. (A) Stochastic divergence, measured as the correlation between replicate realizations of the TSIR model, plotted against community size (logarithmic axis). Black crosses represent the mean across the stochastic realizations of each model. The black line is the logistic regression of mean correlation against log(community size) ($F_{1,58} = 104.4$, $P < 0.01$). (B) Fadeout proportion (percentage of time measles is locally extinct) plotted against community size (logarithmic axis). Red circles represent the observed proportion. The full red line is the logistic regression of observed proportions against log(community size) ($F_{1,58} = 410.6$, $P < 0.01$). Black crosses represent predicted proportions from the stochastic TSIR model (mean across 10 000 realizations). The full black line is the corresponding logistic regression for predicted proportions ($F_{1,58} = 120.9$, $P < 0.01$). (C) Predicted median fadeout length (based on 10 000 stochastic realizations) plotted against the median observed in the time series. The diagonal line represents unbiased predictions.

largest (type I) cities. However, for the remaining cities the deterministic predictions are much less accurate than the stochastic ones. For medium-sized (type II) towns, the deterministic model tends to overestimate the proportion of biennial power. This is probably because of a lack of noise at other frequencies in the simulations, compared to the real epidemics—recall that we do not allow in the simulations for measurement error, or for temporal fluctuations in parameters corresponding to ''environmental'' noise. For small (type III) centers, deterministic models fail to reproduce the power ratio as they predict annual small-amplitude cycles (Fig. 4).

Predictability: stochastic divergence and city size

We can use the TSIR model to study the impact of stochasticity on the measles attractor by looking at the extent to which replicate simulations diverge. Fig. 6a summarizes this effect by plotting the mean correlation among trajectories for each of the 60 cities. The results nicely complement those found through the analyses of power spectra; individual trajectories are almost perfectly correlated for large (type I) cities and the correlation falls to almost zero for small (type III) populations (<100 000). This provides a synoptic illustration of the increasing impact of demographic and extinction–recolonisation stochasticity at low population sizes.

Demographic stochasticity manifests itself through increasing the coefficient of variation of the epidemic birth–death process. An important result of this is local extinction in small populations. Fig. 6b displays the observed proportion of time when measles is locally extinct, compared to the prediction of the doubly stochastic TSIR model. The decline with log(population size) observed in the data is closely matched by the simulated series. The other standard measure of local measles persistence is the incidence of local fadeouts of infection (Bartlett 1960). To allow for spurious zeros due to under-reporting in the data, we defined a fadeout as 3 or more weeks without reported cases. The observed and expected median length of fadeouts are also closely matched between real and simulated series (Fig. 6c).

Nonlinearity and predictability

We cannot fully understand the dynamics of measles by considering the deterministic and stochastic components separately; demographic stochasticity in a linear system would be predicted to push trajectories out of phase even for the largest cities. In order to understand the interaction between the two components we calculate the local Lyapunov exponents (LLEs), be-

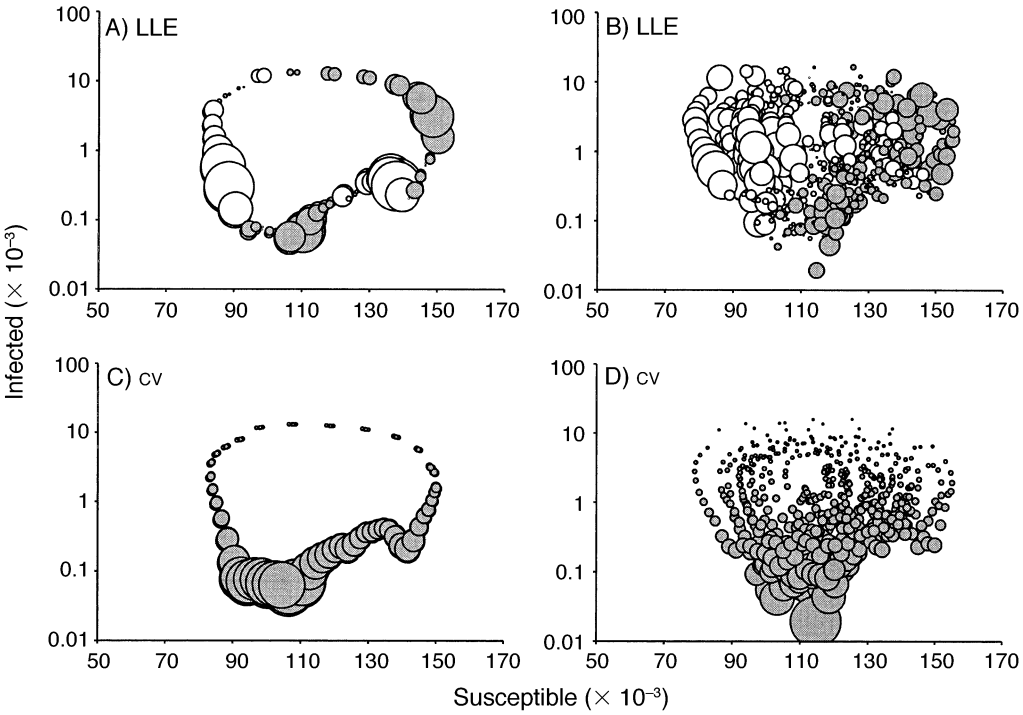

FIG. 7. (A) Local Lyapunov exponents across the biennial attractor predicted for median birth rates in London. Filled circles represent positive values; open circles represent negative values. The area of the circle is proportional to the absolute value of the local LEs (LLEs). The dominant (global) LE is −0.03, despite more than half of the attractor exhibiting positive LLEs (range: −0.21–0.51). (B) LLEs across the observed trajectory of London (1944–1965; see Fig. 1). The median LLE is −0.05 (range: −0.66–0.54). (C) The one-step-ahead coefficient of variation in the nonlinear birth–death process across the attractor depicted in (A). The area of the circle is proportional to the CV. The median CV is 7.3% (range: 1.2–19.6%). (D) The one-step-ahead CV across the observed trajectory of London. The median CV is 4.5% (range: 1.1–32.4%).

cause these allow us to ask how random forces are amplified or decreased across the epidemic cycle. Superimposing the LLEs on the state space representation of the theoretical biennial cycle (Fig. 7a), reveals a complex pattern of noise modulation in measles dynamics. The LLEs are positive during much of the trough phase and the whole of the increase phase of the epidemic. That means that stochastic forces acting during this part of the cycle are, in the short-term, amplified rather than reduced. In contrast, the decrease phase exhibits negative LLEs and hence strong regulation, whereby dynamic noise is quickly reduced in the chain of transmission. The full skeleton, intriguingly, exhibits global contraction (the global Lyapunov exponent is approximately −0.03), even though the proportion of the attractor exhibiting amplification is slightly larger than that exhibiting contraction (Fig. 7a).

With some hesitation, we can repeat the same exercise for the observed trajectory for London. (We need to be careful, because all current understanding, including the present results, indicates that the dynamics of measles in the United Kingdom post-World War II are governed by an attractor that evolves in response to changes in host vital rates). The resultant picture is qualitatively similar to that seen in the idealized biennial attractor. The contraction during the decline phase overcomes the accumulated amplification during the other phases (Fig. 7b).

To complete this exploration of nonlinear predictability, we need to consider how the inherent stochasticity changes across the attractor. Fig. 7c and d depict the magnitude of the demographic stochasticity across phase space for the biennial attractor and the evolving London attractor, respectively. The coefficient of variation is high in the epidemic troughs and declines quickly during epidemic peaks. Note that the decline phase in measles, thus, exhibits both low stochastic forcing and negative LLEs, a very powerful combination that induces tight ''shrinkage'' of any stochastic excursions onto the attractor.

DISCUSSION

As reviewed in the companion paper (Bjørnstad et al. 2002), measles has played a key role both in pure and applied population dynamics and statistical ecology, as well as in the recent flowering of dynamical systems approaches to ecological time series. Bjørnstad et al. (2002) presented a mechanistic modeling framework that unifies these approaches, focusing on how key epidemiological parameters and processes scale with host population size. Here, we have applied the model to investigate a potentially much more difficult

problem—the scaling of long-term dynamics. We aimed to address three questions: first, how well the model captures the dynamics of measles in large cities; second, how do the dynamics and noise scale with population size; third, what is the role of the interaction between noise and regulation in forming the system's predictability. We consider these in turn, then discuss the broader ecological implications of the work.

Long-term dynamics and trends in birth rates

For such a simple formulation, the TSIR model does remarkably well. Based on a 2-wk-ahead fit, it postdicts the essential epidemic dynamics over 20 yr, both qualitatively and quantitatively. Both deterministic and stochastic simulations closely match the well known biennial cycles of measles in the UK (and many other developed countries) during the 1950s and 1960s (Fine and Clarkson 1982, Anderson et al. 1984, Black 1984, Schenzle 1984, Anderson and May 1991, Cliff et al. 1993, Bolker and Grenfell 1995, Grenfell and Harwood 1997). The basic major epidemic dynamics (a ''natural enemy'' interaction between susceptible and infected hosts, forced by seasonality), can also be captured by the model's cousin, the SEIR equations (Schenzle 1984, Bolker and Grenfell 1993, Earn et al. 2000). The SEIR model shows extreme effects of nonlinearity at high seasonal forcing—period-doubling bifurcations to irregular chaotic epidemics at high seasonal amplitude (Aron and Schwartz 1984, Schaffer and Kot 1985, Olsen et al. 1988, Earn et al. 2000). Again, the TSIR echoes these properties of the continuous-time model, with a transition to chaos at high levels of seasonality (Fig. 3).

The TSIR model provides a more natural way than the SEIR to estimate the pattern of seasonality that forces the observed epidemic dynamics. It also automatically allows for changes in birth rate, which generates the observed reverse bifurcation from annual to biennial dynamics at high birth rates (Earn et al. 2000). The clearest illustration of this effect is provided by the strongly annual dynamics for Liverpool (Figs. 2, 4, and 5). Note that this distinctive behavior is predicted to be a result of the greater birth rate in Liverpool—the seasonality and mixing parameters for this city are not different from those in the rest of the 60-town data set (Bjørnstad et al. 2002; see also Finkenstädt et al. 1998). An important area for future work will be to refine the model to capture more accurately the extent and timing of bifurcations in response to birth rate in centers other than London.

A general population dynamic message from our study is that understanding the period of this forced oscillator depends on a proper quantification of both fast (seasonal transmission) and slow (birth rate) changes in the parameters. Predicting the observed nonstationarity in cycle period thus depends in turn on (1) knowing and being able to measure the key ''slow'' variable and (2) having a sufficiently mechanistic understanding of the system. A depressing corollary is that it may be difficult to understand such long-term changes in systems without the unusual level of knowledge available for measles. On a brighter note, the recent development of semi-mechanistic modeling approaches may provide a way forward here (Ellner et al. 1998). It will be interesting to explore whether these methods can capture local spatial dynamics and other variables not currently included in the TSIR model. For example, the fact that the stochastic spectral envelopes in Fig. 4 fail to exactly contain the observed spectra may be due to biases that arise from omitting other biological processes.

Scaling of dynamics and noise

The measles data allow us to investigate, in a uniquely detailed way, the scaling with population size in the relative importance of density-dependent deterministic forces and demographic stochasticity. At first sight, demographic noise is relatively unimportant for measles epidemics in large and medium-sized cities. However, even though the CV of demographic noise is relatively low, it has the potential to drive nontrivial fluctuations around the epidemic cycle (Figs. 1, 2). A dramatic manifestation of this is the potential for noise to push the epidemics from the odd- to the even-year attractor (Fig. 2). This theoretical possibility manifested itself in Norwich (and environs), which exhibited even-year epidemics from 1946 to 1960. Another important effect of stochasticity is well known from theoretical epidemiology—stochastic forcing can excite biennial cycles or even complex dynamics in large and deterministically stable systems (Bartlett 1956, Rand and Wilson 1991). We do not see such effects in the measles data analyzed here, because the strong seasonal forcing drives the system onto a very stable biennial attractor. Note, as a contrast, that whooping cough (another essentially SEIR infection with slightly different parameters) shows a strong response to demographic noise even in large cities (Rohani et al. 1999), as probably does measles in the vaccine era (Earn et al. 2000). It would, hence, be wrong to conclude that demographic stochasticity is trivially unimportant whenever cities are large. Rather it is because prevaccination measles in large cities in England and Wales was governed by an extremely tightly regulated attractor.

Intriguingly, epidemics in large centers appear relatively unaffected by the stochastic perturbations associated with epidemiological coupling to surrounding regions. This reflects how immigration of infection has a negligible effect on the epidemic trajectory as soon as there are more than a handful of resident infecteds in the troughs between epidemics. In the companion paper (Bjørnstad et al. 2002), we show that the influence of an immigrant is $<1\%$ as soon as the resident population of infecteds is >20 individuals. By contrast, the epidemic clockwork in small towns is sensitive both to demographic stochasticity and to the stochastic rate

of influx of infections during fadeout periods. However, once a major epidemic has started, the resulting outbreak is relatively insensitive to stochastic forces even in small cities (see also Bjørnstad et al. 2002). Understanding this ''forest fire''-like effect via multivariate spatial extensions of the TSIR model is a major area for future developments.

The long-term dynamics of the TSIR model generate a range of behaviors, from regular cycles in large centers, via regular epidemics with intervening fadeouts in smaller towns below the CCS, to irregular epidemics with long periods of fadeout in small towns. This gives flesh to Barlett's seminal categorization of type I, II, and III dynamics and the corresponding increase in total fadeouts with decreasing population size. Note, however, that the general pattern of fluctuations is predictable across community sizes, though the exact timing and extent of individual outbreaks is not easy to predict in small host communities where both birth–death and extinction–recolonization stochasticities are dominant. The qualitative predictability of measles dynamics even in small populations echoes the result of the previous paper, that the mean proportion of susceptible ''prey'' in the population is a tightly regulated proportion of the total population size (Bjørnstad et al. 2002). Whether this applies in very small isolated populations (Rhodes and Anderson 1996) is an interesting question for future work. In terms of total fadeouts, we accurately predict the CCS, however, the model somewhat overestimates the length of the fadeouts following local extinction (Fig. 6c). The reason for this divergence is likely to be associated with our assumption that the spatial flux of infection follows a time-invariant Poisson process. In true life, the influx rate is likely to be an, essentially biennially, time-varying process reflecting the aggregate dynamics across the country. This will result in pulsed influx rates that reduce the likelihood of long fadeouts. For example, Keeling and Grenfell (1997) use a version of the SEIR model with biennial imports and a constant infectious period to generate realistic fadeout lengths. We are currently exploring an analogous extension of the TSIR model.

Predictability

In a cogent discussion of epidemic predictability, Cliff (1995) reviews the difficulties of constructing mechanistic or empirical statistical models which predict both the the timing and amplitude of recurrent epidemics. Our results show that the TSIR model has the potential to capture both these characteristics. Overall, the model generates accurate qualitative and (generally) quantitative long-term postdictions of observed prevaccination dynamics of measles in England and Wales. The comparison between model and data is based on a one-step-ahead fit and is therefore not truly out of sample. However, we believe this to be a minor issue, since a model fitted to the latter half of the time series successfully captures the bifurcation to biennial cycles in the first half (not shown). Analyses based on SEIR-like models can also predict qualitative dynamical transitions, driven by birth rate, for data from US cities (Earn et al. 2000). Between-country comparisons of predictability, based on the TSIR model, will be an interesting area for future work, especially as patterns of seasonality in schooling vary between nations.

To understand why large-city measles represents such a predictable system, we examined local Lyapunov exponents across the dynamic attractor. They document a complex interaction between the degree of nonlinearity (as modulated by the strength of seasonal forcing) and noise (controlled mainly by the local abundance of infectives, which in turn are proportional to population size). The most dramatic result is how the stability of the biennial cycle arises from strongly negative LLEs at the end of each major epidemics (Fig. 7). This arises from the powerful contraction in state space caused by the abrupt decline in infectives at the end of the epidemic (Ellner et al. 1998). This ''shrinkage'' results from an abrupt fall in infection rates during the long summer school vacation. The period of maximum dissipation is followed by a period of local expansion and high demographic stochasticity at the nadir of the trough. Intriguingly, the period of strong shrinkage superdominates all other parts of the attractor in the large cities.

We extended the analyses of LLEs to small town dynamics and also to the chaotic trajectories that are induced by high levels of seasonality. In both of these cases, the picture is more complex (Fig. 8). However, they both appear to share a common feature with the biennial epidemic: there is contraction in phase space at the period of faster-than-exponential decline in incidence, towards the end of epidemics. The deterministic chaotic attractor (Fig. 8a) exhibits some additional regions of negative exponents. The TSIR model should allow us in future work to explore how these depend on susceptible and infective densities.

Preliminary analyses (Fig. 8a) suggest that the LLEs of small places do not differ much in magnitude from those of large cities. The qualitative difference in dynamics appears to arise from the increase in stochastic forcing. The large negative exponents at the end of outbreaks suggest local contraction in phase-space that should reduce short-term uncertainty. However, this is a mirage in terms of true predictions, since local extinction of the infection converts the epidemic process into a highly stochastic waiting-time process, during which susceptibles build up until the next ''spark'' of infection. Essentially, therefore, the transition from the epidemic phase to the fadeout phase, corresponds to a shift from a regime where relatively low-dimensional forces are operating to one of more high-dimensional stochastic variation.

On the conceptual side, we feel it appropriate to acknowledge the very interesting recent literature on the meaning of chaos and its hallmark, sensitivity to

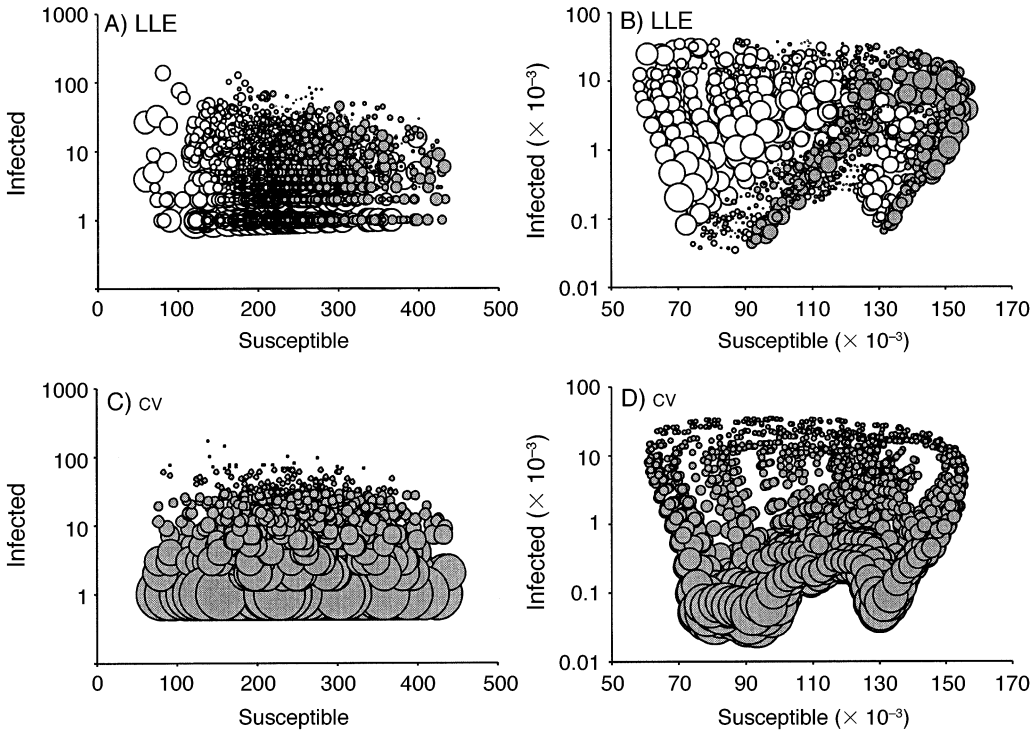

FIG. 8. (A) Local Lyapunov exponents across the stochastic attractor predicted for median birth rates in the smallest city (Teignmouth, 10 000; cf. Fig. 2). Periods of disease extinction have been omitted. Filled circles represent positive values; open circles represent negative vales. The area of the circle is proportional to the absolute value of the LLEs. The mean LLE across the epidemic (nonextinct) part of the attractor is −0.35 (range: −2.94–1.08). (B) LLEs across a chaotic and deterministic attractor (assuming 0.40 in seasonal variation; cf. Fig. 3). The dominant (global) LE is 0.08 (range in LLE: −1.34–1.05). (C) The one-step-ahead coefficient of variation in the nonlinear birth–death process across the attractor depicted in (A). The area of the circle is proportional to the CV. The median CV is 44.73% (range: 7.0–100.0%). (D) The one-step-ahead CV across the chaotic attractor, as depicted in (B). The median CV is 8.2% (range: 0.9–166.6%).

initial conditions, in stochastic systems (Bailey et al. 1997, Tong 1997). A major issue arises because the ''attractor,'' across which we assess mean expansion or contraction, is less clearly defined in stochastic systems (partly because it depends critically on the exact magnitude of the noise). Our study of measles adds to the ecological side of this discussion, by highlighting how ''attractor evolution'' is a dominant feature of this, otherwise extremely stable, system. It is difficult to envisage how to come up with a meaningful measure of mean ''global'' expansion/contraction in the face of such nonstationarity. Fortunately, the advent of local Lyapunov exponents circumvents this problem because they are uniquely defined across phase space and straightforward to interpret across different noise levels and even ''slow'' nonstationarity.

The TSIR model successfully predicts the transition in measles dynamics associated with changes in human birth rates (Figs. 1 and 2). It therefore holds promise as a potential predictive tool in epidemiology, both for childhood infections, such as measles and whooping cough, and perhaps also for infections with more complicated strain structure. An important future test bed for its predictive ability is the dynamics during the more recent vaccination era. Fig. 9 gives a preliminary illustration of this, showing an out-of-sample prediction of the dynamics of measles in London into the vaccine era, based on the fit to the prevaccination time series. Overall, the results show promise, capturing the observed decline in amplitude and the shift away from biennial cycles. However, the TSIR model (especially the deterministic realization) is less good at capturing the irregular and changing period of cylicity into the vaccine era. The variable period probably arises partly from the interaction of noise interacting with increased dynamical complexity caused by vaccination (Earn et al. 2000), combined with variations in epidemiological coupling caused by decorrelation of epidemics (Bolker and Grenfell 1996). Preliminary work (K. Glass and B. Grenfell, *unpublished manuscript*) indicates that we can better capture the interaction of complex dynamics and noise by expressing the transmission exponent, α, as a decreasing function of the recruitment rate of susceptibles, as determined by birth and vaccination rates. We shall also explore the much more irregular prevaccination dynamics of measles seen in some U.S. cities, where preliminary studies indicate a key role for pro-

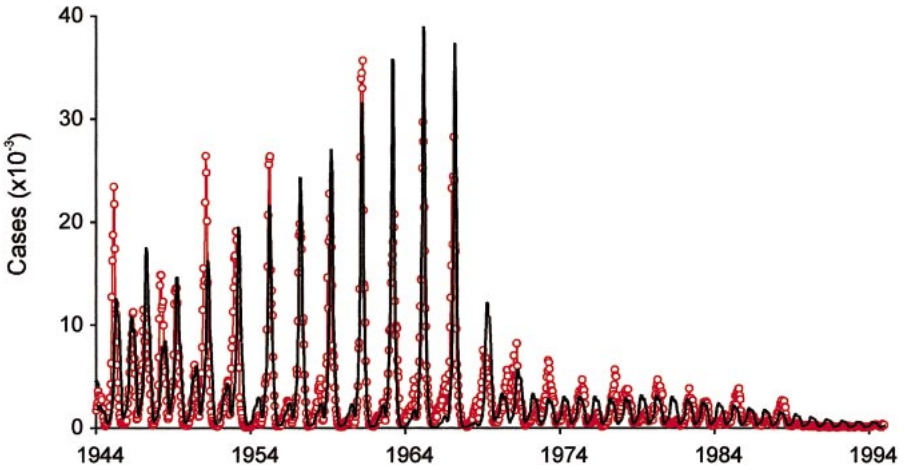

FIG. 9. Use of the TSIR model to predict changes in dynamics into the vaccination era. The model is fitted to the prevaccination time series (1944–1965) and forecasted into the vaccination era by discounting birth rates by the rates of vaccination uptake (Rohani et al. 1999, Earn et al. 2000). Red lines and circles represent observed incidence. The black line is the deterministic forecast.

cess noise and complex dynamics, even in large populations.

Implications for ecological time series analysis

A recent burst of research on ecological time series (Bjørnstad and Grenfell 2001) has emphasized the importance of understanding mechanistically (1) the dimensionality of ecological interactions (Bjørnstad et al. 2001), (2) the balance between density-dependent nonlinearity, process noise, and measurement error (Ellner et al. 1998, Grenfell et al. 1998, Bjørnstad et al. 1999, Meyer and Millar 1999, Millar and Meyer 2000, de Valpine and Hastings 2001), and (3) the importance of spatiotemporal dynamics and coupling (Amarasekare 1998, Swinton 1998, Blasius et al. 1999, Thomas and Kunin 1999). Recent studies also highlight the importance of including seasonality in order to understand ecological dynamics (Leirs et al. 1997, Scheffer et al. 1997, Hansen et al. 1999, King and Schaffer 2001).

Here, we have illustrated that a mechanistic analysis of measles time series allow us to address the methodology and dynamical implications of all these issues.

1) Dimensionality. We have shown that the simple, low-dimensional, TSIR model can capture the long-term dynamical behavior of measles in large cities remarkably accurately. A key reason for this is that the underlying dynamics are effectively a (seasonally forced) two-dimensional interaction between susceptible and infectious individuals. Several previous studies on measles dynamics stressed how age structure is an important component of the transmission dynamics. This would logically imply a much higher dimensionality to the system. However, Earn et al. (2000) show that the high-dimensional age structure of this system can be collapsed onto (a slightly altered) seasonal cycle of transmission. Low-dimensional models have previously been fitted with great success to a variety of data on insect population dynamics (Gurney et al. 1980, Costantino et al. 1997, Dennis et al. 1997). However, these are typically time series from microcosm experiments. One might therefore wonder whether the apparent low dimensionality of the dynamics is an artifact of the laboratory environment. Our study sheds light on this question, showing that even a ''free-ranging'' natural enemy–host system has the potential to adhere to low-dimensional laws. Of course, most ecological interactions are more complex than that between measles and the relatively constant human host populations in developed countries. Recent developments in nonlinear time series methods offer a way to estimate the dimensionality for more complex interactions, and to reconstruct unobserved variables indirectly (Ellner et al. 1998, Bjørnstad et al. 2001, Wood 2001). These methods may prove useful for more complicated free-ranging systems.

2) Scaling noise and nonlinearity. The model can capture the scaling of demographic noise and determinism over three orders of magnitude of population size in this highly nonlinear, nonstationary ecological system. We find that large cities exhibit predictable and highly regulated cycles that are little affected by demographic stochasticity and spatial coupling. Small urban areas, in contrast, exhibit recurrent outbreaks for which a dominant factor is the interepidemic period, as determined by the stochastic import rate. Interestingly, if one were to ignore the scaling of demographic and extinction–recolonization stochasticity and just focus on the dynamic properties of the skeleton, the smallest populations (e.g., Teignmouth; Fig. 8). would be judged to be the more stable and predictable (both the global and local Lyapunov exponents are more negative compared to, say, London). This, of course, is just a detailed illustration of how it is the combined

magnitude of the regulatory and the disruptive forces that is the crucial feature in ecological systems. For measles, the transition from predictable cycles to recurrent outbreaks is—because of it association with a transition in importance of extinction–recolonization dynamics—associated with a shift from local regulation to spatial coupling and metapopulation regulation.

3) Spatial coupling and spatiotemporal dynamics. The shift from local regulation to spatial coupling and metapopulation regulation of smaller population, stress how the regional dynamics of this host–enemy system can only be fully understood as a core–satellite metapopulation (Grenfell and Harwood 1997, Grenfell et al. 2001). Intriguingly, these results parallel the recent emphasis of unstable local dynamics and metapopulation regulation in parasitoid–host systems (Hassell et al. 1991, Murdoch and Briggs 1996, Wilson and Hassell 1997, Amarasekare 1998, 2000). For measles, cyclic lows (epidemic troughs) are the main focus of epidemiologically significant transfer of infection between populations. Strength of coupling, therefore, depends critically on the timing of the sparks of infection from larger centers as well as the overall size of the recipient population. The strength of spatial coupling of this core–satellite metapopulation, therefore, depend not only on movement rates, but also on local dynamics and local host population size. For human infections, understanding this coupling—although more complicated than one might initially think—may turn out to be a relatively tractable exercise, because the relatively clumped spatial population structure of the host is well known.

It will be interesting to see whether the persistence and regulation of other host–natural enemy or predator–prey systems follow the sort of core–satellite metapopulation dynamics we see in measles.

Acknowledgments

B. T. Grenfell and B. F. Finkenstädt were supported financially by the Wellcome Trust. O. N. Bjørnstad was supported by the National Center for Ecological Analysis and Synthesis (a center funded by NSF Grant #DEB-94-21535, the University of California Santa Barbara, and the State of California) and the Norwegian Science Foundation. We thank Ben Bolker, Roger Nisbet, and one anonymous reviewer for valuable comments on the manuscript.

Literature Cited

Amarasekare, P. 1998. Interactions between local dynamics and dispersal: insights from single species models. Theoretical Population Biology **53**:44–59.

Amarasekare, P. 2000. Spatial dynamics in a host–multiparasitoid community. Journal of Animal Ecology **69**:201–213.

Anderson, R. M., B. T. Grenfell, and R. M. May. 1984. Oscillatory fluctuations in the incidence of infectious disease and the impact of vaccination: time series analysis. Journal of Hygiene (Cambridge) **93**:587–608.

Anderson, R. M., and R. M. May. 1991. Infectious diseases of humans: dynamics and control. Oxford University Press, Oxford, UK.

Aron, J. L., and I. B. Schwartz. 1984. Seasonality and period-doubling bifurcations in an epidemic model. Journal of Theoretical Biology **110**:665–679.

Bailey, B. A., S. Ellner, and D. W. Nychka. 1997. Chaos with confidence: asymptotics and applications of local Lyapunov exponents. Pages 115–133 *in* C. Cutler and D. T. Kaplan, editors. Nonlinear dynamics and time series: building a bridge between the natural and statistical sciences. American Mathematical Society, Providence, Rhode Island, USA.

Bailey, N. T. J. 1957. The mathematical theory of epidemics. Griffin, London, UK.

Bartlett, M. S. 1956. Deterministic and stochastic models for recurrent epidemics. Pages 81–109 *in* Proceedings of the Third Berkeley Symposium on Mathematical Statistics and Probability. Volume 4. University of California Press, Berkeley, California, USA.

Bartlett, M. S. 1960. The critical community size for measles in the U.S. Journal of the Royal Statistical Society Series A **123**:37–44.

Bartlett, M. S. 1966. An introduction to stochastic processes, with special reference to methods and applications. Cambridge University Press, Cambridge, UK.

Bjørnstad, O. N., B. Finkenstädt, and B. T. Grenfell. 2002. Dynamics of measles epidemics: estimating scaling of transmission rates using a time series SIR model. Ecological Monographs **72**:169–184.

Bjørnstad, O. N., J.-M. Fromentin, N. C. Stenseth, and J. Gjøsæter. 1999. Cycles and trends in cod population. Proceedings of the National Academy of Science USA **96**: 5066–5071.

Bjørnstad, O. N., and B. T. Grenfell. 2001. Noisy clockwork: Time series analysis of population fluctuations in animals. Science **293**:638–643.

Bjørnstad, O. N., S. M. Sait, N. C. Stenseth, D. J. Thompson, and M. Begon. 2001. Coupling and the impact of specialised enemies on the dimensionality of prey dynamics. Nature **401**:1001–1006.

Bjørnstad, O. N., N. C. Stenseth, T. Saitoh, and O. C. Lingjære. 1998. Mapping the regional transitions to cyclicity in *Clethrionomys rufocanus*: spectral densities and functional data analysis. Researches on Population Ecology **40**:77–84.

Black, F. L. 1984. Measles. Pages 397–418 *in* A. S. Evans, editor. Viral infections of humans: epidemiology and control. Plenum, New York, New York, USA.

Blasius, B., A. Huppert, and L. Stone. 1999. Complex dynamics and phase synchronization in spatially extended ecological systems. Nature **399**:354–359.

Bolker, B. M., and B. T. Grenfell. 1993. Chaos and biological complexity in measles dynamics. Proceedings of the Royal Society of London B **251**:75–81.

Bolker, B. M., and B. T. Grenfell. 1995. Space, persistence and the dynamics of measles epidemics. Philosophical Transactions of the Royal Society of London B **348**:309–320.

Bolker, B. M., and B. T. Grenfell. 1996. Impact of vaccination on the spatial correlation and dynamics of measles epidemics. Proceedings of the National Academy of Science USA **93**:12648–12653.

Cliff, A. D. 1995. Incorporating spatial components into models of epidemic spread. Pages 119–149 *in* D. Mollison, editor. Epidemic models: their structure and relation to data. Cambridge University Press, Cambridge, UK.

Cliff, A. D., P. Haggett, and M. Smallman-Raynor. 1993. Measles: an historical geography of a major human viral disease from global expansion to local retreat, 1840–1990. Blackwell, Oxford, UK.

Costantino, R. F., R. A. Desharnais, J. M. Cushing, and B. Dennis. 1997. Chaotic dynamics in an insect population. Science **275**:389–391.

de Jong, M. C. M., O. Diekmann, and J. A. P. Heesterbeek. 1995. How does transmission of infection depend on population size? Pages 84–94 *in* D. Mollison, editor. Epidemic models: their structure and relation to data. Cambridge University Press, Cambridge, UK.

de Valpine, P., and A. Hastings. 2001. Fitting population models: incorporating noise and observation error. Ecological Monographs **72**:57–76.

Dennis, B., R. A. Desharnais, J. M. Cushing, and R. F. Costantino. 1997. Transitions in population dyanmics: equilibria to periodic cycles to aperiodic cycles. Journal of Animal Ecology **66**:704–729.

Dietz, K., and D. Schenzle. 1985. Mathematical models for infectious disease statistics. Pages 167–204 *in* A. C. Atkinson and S. E. Feinberg, editors. A celebration of statistics. Springer-Verlag, New York, New York, USA.

Earn, D. J. D., P. Rohani, B. M. Bolker, and B. T. Grenfell. 2000. A simple model for complex dynamical transitions in epidemics. Science **287**:667–670.

Eckmann, J.-P., S. O. Kamphorst, D. Ruelle, and S. Ciliberto. 1986. Lyapunov exponents from time series. Physical Review A **34**:4971–4979.

Ellner, S. 2000. Measles as a testbed for characterising nonlinear behaviour in ecology. Pages 1–32 *in* J. N. Perry and R. Smith, editors. Chaos from real data: the analysis of non-linear dynamics in short ecological time series. Academic Press, New York, New York, USA.

Ellner, S. P., B. A. Bailey, G. V. Bobashev, A. R. Gallant, B. T. Grenfell, and D. W. Nychka. 1998. Noise and nonlinearity in measles epidemics: combining mechanistic and statistical approaches to population modelling. American Naturalist **151**:425–440.

Ellner, S., and P. Turchin. 1995. Chaos in a noisy world—new methods and evidence from time-series analysis. American Naturalist **145**:343–375.

Fan, S., M. Gloor, J. Mahlman, S. Pacala, J. Sarmiento, T. Takahashi, and P. Tans. 1998. A large terrestrial carbon sink in North America implied by atmospheric and oceanic carbon dioxide data and models. Science **282**:442–446.

Fine, P. E. M., and J. A. Clarkson. 1982. Measles in England and Wales. I: an analysis of factors underlying seasonal patterns. International Journal of Epidemiology **11**:5–15.

Finkenstädt, B., O. N. Bjørnstad, and B. T. Grenfell. 2002. A stochastic model for extinction and recurrence of epidemics: estimation and inference for measles outbreaks. Biostatistics, *in press*.

Finkenstädt, B. F., and B. T. Grenfell. 1998. Empirical determinants of measles metapopulation dynamics in England and Wales. Proceedings of the Royal Society of London B **265**:211–220.

Finkenstädt, B. F., and B. T. Grenfell. 2000. Time series modelling of childhood diseases: a dynamical systems approach. Journal of the Royal Statistical Society, Series C **49**:187–205.

Finkenstädt, B. F., M. J. Keeling, and B. T. Grenfell. 1998. Patterns of density dependence in measles dynamics. Proceedings of the Royal Society of London B **265**:753–762.

Grenfell, B. T. 2000. Measles as a testbed for characterising nonlinear behaviour in ecology. Pages 47–72 *in* J. N. Perry and R. Smith, editors. Chaos from real data: the analysis of non-linear dynamics in short ecological time series. Academic Press, New York, New York, USA.

Grenfell, B. T., O. N. Bjørnstad, and J. Kappey. 2001. Travelling waves and spatial hierarchies in measles epidemics. Nature **414**:716–723.

Grenfell, B. T., and B. M. Bolker. 1998. Cities and villages: infection hierarchies in a measles metapopulation. Ecology Letters **1**:63–70.

Grenfell, B. T., and A. P. Dobson, editors. 1995. Ecology of infectious diseases in natural populations. Cambridge University Press, Cambridge, UK.

Grenfell, B. T., and J. Harwood. 1997. (Meta)population dynamics of infectious diseases. Trends in Ecology and Evolution **12**:395–399.

Grenfell, B. T., A. Kleczkowski, S. P. Ellner, and B. M. Bolker. 1994. Measles as a case-study in nonlinear forecasting and chaos. Philosophical Transactions of the Royal Society of London A **348**:515–530.

Grenfell, B. T., A. Kleczkowski, S. Ellner, and B. M. Bolker. 1995. Nonlinear forecasting in ecology and epidemiology: measles as a case study. Pages 248–270 *in* H. Tong, editor. Chaos and forecasting. World Scientific, Singapore.

Grenfell, B. T., K. Wilson, B. F. Finkenstadt, T. N. Coulson, S. Murray, S. D. Albon, J. M. Pemberton, T. H. Clutton-Brock, and M. J. Crawley. 1998. Noise and determinism in synchronised sheep dynamics. Nature **394**:674–677.

Gurney, W. S. C., S. P. Blythe, and R. M. Nisbet. 1980. Nicholson's blowflies revisited. Nature **287**:17–21.

Hansen, T. F., N. C. Stenseth, and H. Henttonen. 1999. Multiannual vole cycles and population regulation during long winters: an analysis of seasonal density dependence. American Naturalist **154**:129–139.

Hassell, M. P., H. N. Comins, and R. M. May. 1991. Spatial structure and chaos in insect population dynamics. Nature **353**:255–258.

Henson, S. M., J. M. Cushing, R. F. Costantino, B. Dennis, and R. A. Desharnais. 1998. Phase switching in population cycles. Proceedings of the Royal Society of London B **265**: 2229–2234.

Keeling, M. J., and B. T. Grenfell. 1997. Disease extinction and community size: modeling the persistence of measles. Science **275**:65–67.

Kendall, B. E., W. M. Schaffer, and C. W. Tidd. 1993. Transient periodicity in chaos. Physics Letters A **177**:13–20.

Kendall, D. G. 1949. Stochastic processes and population growth. Journal of Royal Statistical Society B **11**:230–264.

King, A. A., and W. M. Schaffer. 2001. The geometry of a population cycle: a mechanistic model of snowshoe hare demography. Ecology **58**:835–859.

Leirs, H., N. C. Stenseth, J. D. Nichols, J. E. Hines, R. Verhagen, and W. Verheyen. 1997. Stochastic seasonality and nonlinear density-dependent factors regulate population size in an African rodent. Nature **389**:176–180.

Liu, W. M., H. W. Hethcote, and S. A. Levin. 1987. Dynamical behavior of epidemiological models with nonlinear incidence rates. Journal of Mathematical Biology **25**:359–380.

May, R. M. 1973. Stability and complexity in model ecosystems. Princeton University Press, Princeton, New Jersey, USA.

McCallum, H., N. Barlow, and J. Hone. 2001. How should pathogen transmission be modelled? Trends in Ecology and Evolution **16**:295–300.

Meyer, R., and R. B. Millar. 1999. BUGS in Bayesian stock assessments. Canadian Journal of Fisheries and Aquatic Sciences **56**:1078–1086.

Millar, R. B., and R. Meyer. 2000. Bayesian state-space modeling of age-structured data: fitting a model is just the beginning. Canadian Journal of Fisheries and Aquatic Sciences **57**:43–50.

Mollison, D., editor. 1995. Epidemic models: their structure and relation to data. Cambridge University Press, Cambridge, UK.

Murdoch, W. W., and C. J. Briggs. 1996. Theory of biological control: recent developments. Ecology **77**:2001–2013.

Murdoch, W. W., and E. McCauley. 1985. Three distinct types of dynamic behaviour shown by a single planktonic system. Nature **316**:628–630.

Nisbet, R. M., and W. S. C. Gurney. 1982. Modelling fluctuating populations. Wiley, Chichester, UK.
Olsen, L. F., G. L. Truty, and W. M. Schaffer. 1988. Oscillations and chaos in epidemics: a nonlinear dynamic study of six childhood diseases in Copenhagen, Denmark. Theoretical Population Biology **33**:344–370.
Priestley, M. B. 1982. Time series analysis and forecasting. Second edition. Academic Press, London, UK.
Rand, D. A., and H. Wilson. 1991. Chaotic stochasticity: a ubiquitous source of unpredictability in epidemics. Proceedings of the Royal Society of London B **246**:179–184.
Renshaw, E. 1991. Modelling biological populations in space and time. Cambridge University Press, Cambridge, UK.
Rhodes, C. J., and R. M. Anderson. 1996. Power laws governing epidemics in isolated populations. Nature **381**:600–602.
Rohani, P., D. J. D. Earn, and B. T. Grenfell. 1999. Opposite patterns of synchrony in sympatric disease metapopulations. Science **286**:968–971.
Royama, T. 1992. Analytical population dynamics. Chapman and Hall, London, UK.
Schaffer, W. M., B. E. Kendall, and C. W. Tidd. 1993. Transient periodicity and episodic predictability in biological dynamics. IMA Journal of Mathematics Applied in Medicine and Biology **10**:227–247.
Schaffer, W. M., and M. Kot. 1985. Nearly one dimensional dynamics in an epidemic. Journal of Theoretical Biology **112**:403–427.
Scheffer, M., S. Rinaldi, Y. A. Kuznetsov, and E. H. Van Nes. 1997. Seasonal dynamics of Daphnia and algae explained as a periodically forced predator–prey system. Oikos **80**: 519–532.
Schenzle, D. 1984. An age-structured model of pre- and post-vaccination measles transmission. IMA Journal of Mathematics Applied in Medicine and Biology **1**:169–191.
Stenseth, N. C., O. N. Bjørnstad, and T. Saitoh. 1996. A gradient from stable to cyclic populations of *Clethrionomys rufocanus* in Hokkaido, Japan. Proceedings of the Royal Society of London B **263**:1117–1126.
Stokes, T. K., W. S. C. Gurney, R. M. Nisbet, and S. P. Blythe. 1988. Parameter evolution in a laboratory insect population. Theoretical Population Biology **34**:248–265.
Sugihara, G. 1995. Ecology—from out of the blue. Nature **378**:559–560.
Sugihara, G., B. Grenfell, and R. M. May. 1990. Distinguishing error from chaos in ecological time series. Philosophical Transactions of the Royal Society of London B **330**:235–251.
Sugihara, G., and R. M. May. 1990. Nonlinear forecasting as a way of distinguishing chaos from measurement error in time series. Nature **344**:734–741.
Swinton, J. 1998. Extinction times and phase transitions for spatially structured closed epidemics. Bulletin of Mathematical Biology **60**:215–230.
Thomas, C. D., and W. E. Kunin. 1999. The spatial structure of populations. Journal of Animal Ecology **68**:647–657.
Tidd, C. W., L. F. Olsen, and W. M. Schaffer. 1993. The case for chaos in childhood epidemics: II. Predicting historical epidemics from mathematical models. Proceedings of the Royal Society of London B **254**:257–273.
Tong, H. 1990. Non-linear time series: a dynamical systems approach. Oxford University Press, Oxford, UK.
Tong, H. 1997. Some comments on nonlinear time series analysis. Pages 17–27 *in* C. Cutler and D. T. Kaplan, editors. Nonlinear dynamics and time series: building a bridge between the natural and statistical sciences. American Mathematical Society, Providence, Rhode Island, USA.
Wilson, H. B., and M. P. Hassell. 1997. Host–parasitoid spatial models: the interplay of demographic stochasticity and dynamics. Proceedings of the Royal Society of London B **264**:1189–1195.
Wood, S. N. 2001. Partially specified ecological models. Ecological Monographs **71**:1–25.